https://doi.org/10.5194/acp-2022-316
Preprint. Discussion started: 2 June 2022

Atmospheric Chemistry and Physics Discussions

Record-breaking statistics detect islands of cooling in a sea of warming

Elisa T. Sena[1], Ilan Koren[2], Orit Altaratz[2], Alexander B Kostinski[3]

[1]Multidisciplinary Department, Federal University of São Paulo, São Paulo, Brazil
[2]Department of Earth and Planetary Sciences, Weizmann Institute of Sciences, Rehovot, Israel
[3]Department of Physics, Michigan Technological University, Houghton, USA

Correspondence to: Ilan Koren (ilan.koren@weizmann.ac.il)

Abstract. Record-breaking statistics are combined here with geographic mode of exploration to construct a new object: a record-breaking map. Such maps are shown here to reveal surprisingly robust statistical results and spatial content. Specifically, we examine a time series of sea surface temperature (SST) values and show that high SST records have been broken far more frequently than the expected rate for a trend-free random variable (TFRV) over the vast majority of oceans (83% of the grid cells). This, together with the asymmetry between high and low records and their deviation from a TRFV, indicate SST warming over most oceans, obtained by using a general and simple-to-use method. The spatial patterns of this warming are coherent and reveal islands of cooling, such as the "cold blob" in the North Atlantic and a surprising elliptical area in the Southern Ocean, near the Ross sea gyre, not previously reported.

1 Introduction

Man-made greenhouse gas (GHG) emissions have caused staggering changes to the climate system (Masson-Delmotte, 2021), made evident by trends in various types of observations, including i) an increasing trend in the mean global temperature and ocean heat content (Hansen et al., 2010, Cheng et al., 2017); ii) sea-level rise, mostly due to the thermal expansion of the oceans and, to a lesser extent, due to ice melting over land (Llovel et al., 2019, Watson et al., 2015, Dangendorf et al., 2017), and iii) the elevated frequency and intensity of extreme events, and land and marine heatwaves (Alexander, et al., 2016, Pendergrass and Hartmann, 2014, Myhre et al., 2019, Frölicher et al, 2018, Laufkötter et al., 2020, Oliver et al., 2018).

Nevertheless, the analysis of climatological time series poses many challenges to quantitative trend extraction because probability distributions of climatological variables are usually not known a priori (Wilcon 2003, Ghil et al., 2002, Gluhovsky and Agee, 2007), non-linearity effects arise from the complex processes and mechanisms involved, and the entanglement of natural and anthropogenic effects obscures true trends in short time series. Besides these factors, climatological time series are often composed of datasets measured by different instruments (satellites, for example) or use slightly different measuring methodologies, which may lead to discontinuities, among other problems. All these factors point

https://doi.org/10.5194/acp-2022-316
Preprint. Discussion started: 2 June 2022


Atmospheric Chemistry and Physics Discussions

to the need to pursue robust distribution-invariant ways of extracting trends from intermittently sampled climatological time series, and record-breaking statistics is one such approach (e.g., Anderson and Kostinski, 2011).

Unlike extreme value statistics, which is not concerned with the position of the observations in the time series, in record-breaking statistics, this information is crucial, rendering trend detection possible. In their seminal 1954 paper, Foster and Stuart used the asymmetry between low and high records to identify trends and variance in time series, using examples of athletics and meteorological data. Since then, this technique, along with various improvements, has been applied to answer a myriad of questions related to the statistical behavior of time series in finance (Wergen et al., 2011), geophysics (Yoder et al., 2010, Van Aalsburg et al., 2010), climate (Benestad, 2004, Redner and Petersen, 2006), and many other fields (Krug and Jain, 2005, Shcherbakov et al., 2013). Some examples of applications of record-breaking statistics in climatological time series are the study of trends, variability, stationarity, and independence in surface temperature (Anderson and Kostinski, 2010; 2011; 2016; Kostinski and Anderson, 2014), rainfall (Lehmann et al., 2015; 2018), and flood events (Vogel et al., 2001). The advantages of this method are its simplicity and generality. Since only serial ordering matters, the method is not limited to linear trends. It is robust insofar as it is distribution-invariant, unit-insensitive (independent of magnitude), handles non-uniform or intermittent sampling, and is non-parametric. Moreover, when applied together with spatial information (as is done in this work), such analysis easily detects spatial structures of trends and their significance. This can be useful for analyzing the statistics of climate variables.

Sea surface temperature (SST) is one of the most important and well-sampled physical properties of the ocean, describing the important interface between the ocean and the lower atmosphere. Ocean-atmosphere interactions are key processes in the climate system, affecting energy, moisture, and particle fluxes. The ocean stores energy, distributes heat and moisture, and drives weather systems. Long-term measurements of global SST are readily available from climate archives, allowing an analysis of large-scale trends (Huang et al., 2017, Alexander et al., 2018). We use record-breaking statistics to explore local trends and identify their spatial patterns in 75 years of global SST data (from 1946 to 2020), a variable that has been shown to increase over time (Wuebbles et al., 2017, Hartmann et al., 2013), using linear regression analysis. The use of record-breaking statistics, presented below, has not been applied to SST data analysis, to the best of our knowledge.

To identify excess or deficits in the records, which are good trend indicators, the observed number of records is scaled by the expected value calculated for a trend-free random variable (TFRV). The asymmetry between the number of high and low records is another metric employed here to assess a trend in the mean value of the time series. The results are discussed for different oceanic regions, and the spatial patterns of record-breaking are examined. The deviation of the observed number of records from the expected value (in units of standard deviation) is used to gauge the significance of the results. Similar analyses can be performed on many other key climatological variables to explore their trends and significance.

https://doi.org/10.5194/acp-2022-316
Preprint. Discussion started: 2 June 2022

Atmospheric Chemistry and Physics Discussions

2 Methods

2.1 A brief summary of the record-breaking theory

For a given time series of a random variable (x), the likelihood of breaking a record at the nth element is equal to the likelihood that all the preceding values in this time series are smaller than it. Therefore, if the time series is of a trend-free, independently drawn random variable (TFRV), the likelihood of breaking a record decreases monotonically with n. The first sample is defined to be record-breaking. For a TFRV (arbitrary distribution), the probability that the second sample will be higher than the first is ½, for the 3rd to be higher than the first two is 1/3, etc. Accordingly, the probability for the nth variable is:

$$P(n) = \max(x_1, \dots, x_n)) = \frac{1}{n}. \qquad (1)$$

Therefore, the expected number of records after n time steps, *H(n)*, is given by:

$$H(n) = \sum_{i=1}^{n} P(i) = 1 + \frac{1}{2} + \frac{1}{3} + \dots + \frac{1}{n}. \qquad (2)$$

H(n) is the expected average number of records that numerous TFRV data vectors of length *n* will converge to. The complete distribution of records is a function of all possible permutations for record-breaking sequences. Arnold et al. (2011) have shown that the exact probability of a TFRV to break k records in a time series of length n is given by the unsigned Stirling number of the first kind divided by the factorial of the time series length:

$$P(k) = \frac{|S(n,k)|}{n!}, \qquad (3)$$

where $|S(n,k)|$ are the coefficients of x^k in a rising factorial of *n* terms, that is,

$$\prod_{i=1}^{n}(x + i - 1) = \sum_{k=0}^{n}|S(n,k)|x^k\,. \qquad (4)$$

A complete description of the Stirling numbers and how to calculate them using a recurrence relation can be found in e.g., Jordan (1950).

Glick (1978) used an indicator function, replacing the random vector $\boldsymbol{x(n)}$ with a binary function $\boldsymbol{y(n)}$ that counts record-breaking events. $\boldsymbol{y(n)}$ is zero everywhere but on $\boldsymbol{x_i}$ samples that break the record of all samples before them. Therefore, the mean of the $\boldsymbol{i^{th}}$ sample, $\boldsymbol{E(y_i) = \frac{1}{i}}$, and the variance can be calculated directly as $\boldsymbol{V(y_i) = E(y_i^2) - E(y_i)^2}$, namely $\boldsymbol{V(y_i) = \frac{1}{i} - \frac{1}{i^2}}$. Since there are no correlations between any pair of the $\boldsymbol{y_i}$ -s, the sum of $\boldsymbol{y_i}$ that measures the average expectations for the number of $\boldsymbol{x_n}$ breaking is, as expected, $\boldsymbol{H(n) = \sum_{i=1}^{n}\frac{1}{i}}$ and the variance $\boldsymbol{V(n) = V(x_n)}$ is simply the sum of all $\boldsymbol{y_i}$ variances:

$$V(n) = \sum_{i=1}^{n}\frac{1}{i} - \sum_{i=1}^{n}\frac{1}{i^2} \qquad (5)$$

https://doi.org/10.5194/acp-2022-316
Preprint. Discussion started: 2 June 2022


Atmospheric Chemistry and Physics Discussions

By knowing the expected mean and variance for the TFRV number of record-breaking events, one can estimate the magnitude and significance of the deviations from them.

In this work, we present 'record-breaking maps' that provide information on the geographical structure of SST trends.

2.2 Significance assessment with the Kolmogorov-Smirnov test

The collective significance of SST trends over the entire globe was assessed by the one-sample non-parametric Kolmogorov-Smirnov (KS) test. For that, the CDF of the observed number of records was compared with the TFRV theoretical distribution from Eq. (3). The maximum distance D between the CDFs was used to infer the significance of the observed records. We compared the observed D values with the distribution of D values obtained by applying the KS test to 3000 CDFs obtained from three million Monte Carlo simulations of TFRV records, 75 samples long each. A detailed explanation of how to calculate the significance using the KS test is provided in Glienke et al. (2020).

2.3 Data

The method is applied to 3D datasets in which the horizontal x and y indices represent the location (longitude and latitude), and the third dimension is the time of the sea surface temperature (SST) measurement. We treat each pixel as an independent time series and estimate the deviations from randomness.

The dataset used in the analyses comprises the monthly global estimates of SST from NOAA's extended reconstructed sea surface temperature, version 5 (NOAA-ERSST-v5), from 1946 to 2020 (Huang et al., 2017). It is a combination of in situ observations from ships, buoys, and Argo floats above 5 meters, and the Hadley Centre version 2 ice-SST concentration (HadISST-v2) derived from the International Comprehensive Ocean-Atmosphere Dataset (ICOADS) Release 3.0. Based on monthly error estimates (Huang et al., 2016), the SST annual mean error was set at 0.1ºC. To avoid many ties, pixels covered by more than 90% of sea ice were excluded from the analysis, as in this case, the SST is set to the freezing point temperature of -1.8ºC. Although this dataset provides SST estimates since 1854 in a 2º x 2º grid resolution, the analysis period was restricted to 1946 until the present to avoid biases and artifacts due to bucket design, different measurement approaches, and data truncation that resulted in spurious SST measurements, especially by Japanese and German ships before the end of World War II (Chan et al., 2019). This dataset is being continuously improved and current and previous versions have already been applied to infer SST trends (e.g., Deser et al., 2010, Wuebbles et al., 2017, Chan et al., 2019).

3 Results

The record-breaking maps of the observed number of high and low records of SST during the 75-years of the study period are presented in Fig. 1a,b. To illustrate the procedure, we chose time series of annual mean SST for two pixels located in points A (0ºN; 95ºE) and B (40ºN; 195ºE) (panels 1c and 1d). High and low records of SST are marked with red and blue

https://doi.org/10.5194/acp-2022-316
Preprint. Discussion started: 2 June 2022


Atmospheric Chemistry and Physics Discussions

dots, respectively. There is an increasing trend at point A, with 15 high records and 3 low records. In contrast, point B series presents more low than high records, i.e., 7 vs. 4, respectively. This asymmetry is further explored by using the number of records to gauge trends in the SST and identify their spatial patterns.

Some simple metrics proposed by Foster and Stuart (1954) and Anderson and Kostinski (2011), may be used as indicators of possible trends in the time series of highly variable data. One such metric is obtained simply by dividing the number of observed records, $R(n)$, by the expected number of records for a TFRV, $H(n)$. The ratio $R(n)/H(n)$ can be used to quantify by how much the observed number of records exceeds or falls short of the TFRV expectation for both the high and low records. In addition to the previous indicators, the asymmetry between the number of high and low records can also be used as a metric for the time series trend. Here, we use the natural logarithm of the ratio between R_{High} and R_{Low} as a trend indicator to complement the previous analyses (Anderson and Kostinski, 2011),

$$\rho = ln\left(\frac{R_{High}}{R_{Low}}\right). \quad (6)$$

ρ distinguishes between increasing and decreasing trends, and its magnitude is related to the slope of the curve. These tests explore different aspects of the record-breaking statistics and offer additional support for the presence of a trend in noisy data.

The record-breaking maps of the observed number of high and low SST records over the TFRV expected number of records ($R(n)/H(n)$), the trend indicator index $\boldsymbol{\rho}$ (Eq. 6)**,** and their frequency distributions are shown in Fig. 2. The red (blue) color in the maps indicates excess (deficit) of high records in panel a, deficit (excess) of low records in panel c, and positive (negative) values of $\boldsymbol{\rho}$ in panel e. The contrast between the distributions of the high and low records is evident. The expected number of records for a TFRV time series of length 75 is ~5. As Figs. 1 and 2 demonstrate, for most of the global oceans, the observed number of high records far exceeds the TFRV expected value of 5, while for the low records, it is below 5 in most pixels. In 83% of the grid cells, the number of high records is above the expected, and in 17% it is more than twice the expected value for a TFRV. It is particularly evident in the tropical and subtropical Atlantic, the Central Pacific, the Eastern Indian Ocean, and the Southern sea. Conversely, the number of low records seldom exceeds the TFRV expected value by more than twice (less than 0.1% of the pixels), and $R_{Low}(n)/H(n)$ is below 1 in more than 72% of the grid cells. Fig. 2c depicts the trend indicator index $\boldsymbol{\rho}$. Positive values of $\boldsymbol{\rho}$ are observed over most of the globe. The ratio between high and low records is higher than 1 in 88% of the globe, and higher than 2 in 51% of the pixels. This asymmetry in the number of high and low records is a good indicator of a trend in the SST. It is interesting to notice that, even though the overwhelming majority of the oceanic area is warming (as evidenced by the predominance of the red color in all record-breaking maps), there are some islands of consistent cooling (where the spatial patterns show a coherent persistence of the color blue in many neighboring pixels). We will discuss some of the most interesting cooling islands' features in the next section.

We also examined differences in regional trends (the regions are marked in Fig. 1b). Fig. 3 presents box plots of the distribution of high and low SST records over the expected TFRV value ($R(n)/H(n)$) and of $\boldsymbol{\rho}$ for each region. Once again, the results confirm the asymmetry between the number of high and low records. The global distribution of high records is

https://doi.org/10.5194/acp-2022-316
Preprint. Discussion started: 2 June 2022


Atmospheric Chemistry and Physics Discussions

shifted to the right (towards higher values) compared to the expected distribution of records for a TFRV. All regions show an excess of high records compared to both the expected value for a TFRV and to the number of low records. The asymmetry between the number of high and low records is evident in all oceanic regions since the medians of the distribution of the observed high (low) records were higher (lower) than 1 in all of them (Figs. 3a and 3b). The Arctic, Indian, South Pacific, South and North Atlantic Oceans are the regions where the excess of high records is more prominent, all of them exhibiting values of over 75% above the expected number (Fig. 3a). The South Atlantic ocean maintains the highest ratio between high and low records (Fig. 3c). These results further confirm the global extent of the positive trend in SST; global warming of the oceans.

Are the number of records observed in the global SST 75-year time series significantly different from those calculated for a TFRV time series of the same length? To answer this question, Fig. 4 compares the cumulative distribution of the observed number of high (red) and low (blue) records of all the pixels (over the whole globe) with the theoretical TFRV distribution of records (green). It is clear that the number of high records is always larger than the one for the theoretical distribution; that is, the observed curve is shifted to the right compared to the theoretical one. The opposite behavior is observed for the number of low records. The Kolmogorov-Smirnov (KS) test indicates that the maximum distance D between the distribution of observed high (low) records and the theoretical cumulative distribution function (CDF) of the number of records expected for a TRFV (Eq. 3) is DH=0.32 (DL=0.31). To assess the significance of the D values obtained for the observed records, the KS test was applied on 3000 CDFs of the number of records obtained for TFRV Monte Carlo simulations. The probability distribution function (PDF) of the maximum distance D for the Monte Carlo simulations is shown in Fig. 4c. The green dashed line shows the 99.9% percentile ($D_{99.9}$), and the maximum deviations, DH and DL, are highlighted in red and blue dashed lines, respectively. The results show that the observed DH and DL are overwhelmingly significant, both about 6 times $D_{99.9}$, the distance expected for the 99.9% percentile of the Monte Carlo simulations' PDF. Thus, the global ocean SST does not represent a TFRV, and warming is evident.

Having established the global (bulk) significance of SST trends, we next consider the local significance in order to explore spatial patterns. To that end, for each 2º by 2º pixel of the grid, we analyzed the deviation from expectation in standard deviation units, given by the difference between the observed number of records, R(n), and the expected number of records, H(n), for a TFRV, divided by the theoretical standard deviation, $\boldsymbol{\sigma} = \sqrt{\mathbf{V(n)}}$, where *V(n)* is the variance of the TFRV distribution,

$$\boldsymbol{Dev} = \frac{\mathbf{R(n)-H(n)}}{\boldsymbol{\sigma}}. \quad (7)$$

The record-breaking maps in Fig. 5 show that in 15.8% of the pixels, the number of high records exceeds the expected TFRV value by more than 2 standard deviations, about 12 times as many pixels as for TFRV. In about 2.4% of the pixels, it is above 3 standard deviations, in contrast to a TFRV value of (virtually) zero. We note the clear positive record-breaking trend over almost the entire Atlantic Ocean (except for high latitudes in the northern hemisphere), the tropical Pacific Ocean, and most

https://doi.org/10.5194/acp-2022-316
Preprint. Discussion started: 2 June 2022


Atmospheric Chemistry and Physics Discussions

of the Indian Ocean (especially near India and Western Australia). These positive regional anomalies are more comprehensively addressed below.

The low records show large deviations from TFRV in the Arctic region, in the North and South Atlantic, and in some regions of the Indian and Pacific Oceans (where the colors are dark red, signaling fewer records than expected). The histograms in panels 5c and 5d show $\boldsymbol{Dev}$ values as high as 6 for high records and 3 for low records. Although the associated theoretical PDF of the number of records for a TFRV is asymmetric, the difference between the mean and the median of the distribution for 75 observations is very small (4.9 and 5, respectively). Therefore, using the normal approximation, the deviations displayed in Fig. 3 are again highly significant and demonstrate that the number of records of the SST time series of each pixel is far from that calculated for a TFRV. For example, a 2-standard-deviation value would be very unlikely for the theoretical distribution of the records of a TFRV time series, being above the 95th percentile.

4 Discussion

This work uses record-breaking statistics for identifying trends in a global dataset of SST time series (between 1946 and 2020) and explores their spatial patterns. This method has many advantages, and it is free from assumptions on the distribution. The record-breaking maps allow for both estimating the existence and significance of trends locally (per pixel, see Figs. 2 and 5 as examples) and revealing spatial structures (such as areas with significantly strong trends or, in contrast, areas with opposite trends). These spatial patterns can hint at the geophysical processes controlling the explored variable. This method is particularly well-suited for datasets consisting of many but relatively short time series, as is often the case in climatology.

https://doi.org/10.5194/acp-2022-316
Preprint. Discussion started: 2 June 2022


Atmospheric Chemistry and Physics Discussions

The asymmetry between the numbers of high and low records and their deviation from the theoretical calculation for a TRFV indicate a significant increasing trend in SST over most of the Oceans but also expose some cooling regions (Figs. 2-5). Comparing panels 2a and 2c reveals extensive warming regions, associated with large numbers of high records and small numbers of low records, in the tropical and mid-latitude Northern Atlantic Ocean, the whole South Atlantic Ocean, south of Australia, in the vicinity of Indonesia (in the Indian Ocean), and near the west coast of Mexico (in the Pacific Ocean). Despite the overwhelming warming, coherent cooling patterns are also observed in regions characterized by a small number of high records (Fig. 2a) and a large number of low records (Fig. 2c). Some of the regions where low records were broken more frequently (like in the tropical eastern Pacific and in the Indian Ocean) may be associated with strong events of the negative phase of natural climate oscillations like El Niño Southern Oscillation (ENSO) and the Indian Ocean Dipole (IOD) in the Southern Hemisphere. Previous observations that showed cooling in part of the North Atlantic Ocean followed by warming in the last two decades (Deser et al., 2010) are consistent with the maps in Fig. 2. Also noteworthy are the large spatial clusters that show the same trend signals, proving the consistency in the spatial correlations of *R(n)/H(n)*. Next, we focus on some interesting islands of cooling, such as the high latitudes of the Northern Atlantic, near Greenland, some areas in the North Pacific, and, even more interestingly, in the Southern Ocean between Australia and South America.

The cooling observed here in the North Atlantic region is consistent with a phenomenon known as "the cold blob", a region in the ocean near Greenland that has been experiencing cooling over the years despite global warming. The causes for this cooling have been associated with ice melting in high latitudes that induces changes in the ocean circulation due to increased freshwater fluxes, causing a slowdown of the Atlantic Meridional Overturning Circulation (AMOC) and reduced heat transport to that region (Josey, et al., 2018, Rahmstorf et al., 2015). More recently, other factors, such as heat transport out of the "cold blob" to higher latitudes and increased cloudiness over the area, have also been linked to the cooling in this region (Keil et al., 2020). The causes of such cooling have been linked to human footprint, mainly the anthropogenic release of greenhouse gases into the atmosphere, as opposed to natural variability (Chemke et al., 2020). A similar cooling pattern is observed here near Antarctica, around longitude 200º. Cooling in the surface of the Southern Ocean and warming of the subsurface have been previously reported (Masson-Delmotte, 2021, Haumann et al., 2020). However, unlike previous findings, in the present analysis, the cooling trend seems to appear in a very specific geographical spot, i.e., near the Ross gyre (Fig. 2). The mechanisms associated with such cooling are still under investigation. Upwelling delays the warming of the sea surface but cannot explain the cooling. Haumann et al. (2020) proposed that the cooling is due to wind-driven sea-ice transport and its subsequent melting, decreasing the salinity of the upper ocean. Freshening of the upper ocean weakens convection and vertical mixing, preventing the warming of the ocean surface (Armour et al., 2016). Finally, the cooling pattern in the North Pacific is not as consistent as the other ones. The time series in this region presents an SST increase until around the 1980s and then a decrease. Analyzing SST from observations and models, Deser et al. (2010) found a low significance of trends in this region. The analysis performed here shows that record-breaking statistics is a powerful tool capable of detecting trends in noisy global time series and demonstrates how to evaluate their significance in climate science studies.

https://doi.org/10.5194/acp-2022-316
Preprint. Discussion started: 2 June 2022

Atmospheric Chemistry and Physics Discussions

Acknowledgment

This project has received funding from the European Research Council (ERC), under the European Union's Horizon 2020 research and innovation programme (CloudCT, grant agreement No 810370). E. T. S. also acknowledges CNPq Universal Project grant 421870/2018-4, and A. B. K. thanks NSF grant AGS-1639868. We thank NOAA/OAR/ESRL PSL, Boulder, Colorado, USA, for processing and maintaining the NOAA_ERSST_V5 data in their website.

References

Alexander, L. V. Global observed long-term changes in temperature and precipitation extremes: A review of progress and limitations in IPCC assessments and beyond. Weather and Climate Extremes 11, 4–16, https://doi.org/10.1016/j.wace.2015.10.007, 2016.

Alexander, M.A., Scott, J.D., Friedland, K.D., Mills, K.E., Nye, J.A., Pershing, A.J., Thomas, A.C. and Carmack, E.C., Projected sea surface temperatures over the 21st century: Changes in the mean, variability and extremes for large marine ecosystem regions of Northern Oceans. Elementa: Science of the Anthropocene, 6, https://doi.org/10.1525/, 2018.

Anderson, A. and Kostinski, A., Evolution and distribution of record-breaking high and low monthly mean temperatures. Journal of applied meteorology and climatology, 50(9), pp.1859-1871, 2011.

Anderson, A. and Kostinski, A., Reversible record breaking and variability: Temperature distributions across the globe. Journal of applied meteorology and climatology, 49(8), pp.1681-1691, 2010.

Anderson, A. and Kostinski, A., Temperature variability and early clustering of record-breaking events. Theoretical and Applied Climatology, 124(3), pp.825-833, 2016.

Armour, K.C., Marshall, J., Scott, J.R., Donohoe, A. and Newsom, E.R., Southern Ocean warming delayed by circumpolar upwelling and equatorward transport. Nature Geoscience, 9(7), pp.549-554, 2016.

Arnold, B.C., Balakrishnan, N. and Nagaraja, H.N., Records (Vol. 768). John Wiley & Sons, 2011.

Benestad, R.E., Record-values, nonstationarity tests and extreme value distributions. Global and Planetary Change, 44(1-4), pp.11-26, 2004.

Chan, D., Kent, E.C., Berry, D.I. et al. Correcting datasets leads to more homogeneous early-twentieth-century sea surface warming. Nature 571, 393–397, https://doi.org/10.1038/s41586-019-1349-2, 2019

Chemke, R., Zanna, L. and Polvani, L.M., Identifying a human signal in the North Atlantic warming hole. Nature communications, 11(1), pp.1-7, 2020.

Cheng, L., Trenberth, K.E., Fasullo, J., Boyer, T., Abraham, J. and Zhu, J., Improved estimates of ocean heat content from 1960 to 2015. Science Advances, 3(3), p.e1601545, 2017.

Dangendorf, S., Marcos, M., Wöppelmann, G., Conrad, C.P., Frederikse, T. and Riva, R. Reassessment of 20th century global mean sea level rise. Proceedings of the National Academy of Sciences, 114(23), pp.5946-5951, https://doi.org/10.1073/pnas.1616007114, 2017.

https://doi.org/10.5194/acp-2022-316
Preprint. Discussion started: 2 June 2022


Atmospheric Chemistry and Physics Discussions

Deser, C., Phillips, A.S. and Alexander, M.A., Twentieth century tropical sea surface temperature trends revisited. Geophysical Research Letters, 37(10), 2010.

Foster, F.G. and Stuart, A., Distribution-Free Tests in Time-Series Based on the Breaking of Records Division of Research Techniques, London School of Economics. Journal of the Royal Statistical Society: Series B (Methodological), 16(1), pp.1-13, 1954.

Frölicher, T.L., Fischer, E.M. & Gruber, N. Marine heatwaves under global warming. Nature, 560, 360–364. https://doi.org/10.1038/s41586-018-0383-9, 2018.

Ghil, M., Allen, M.R., Dettinger, M.D., Ide, K., Kondrashov, D., Mann, M.E., Robertson, A.W., Saunders, A., Tian, Y., Varadi, F. and Yiou, P., Advanced spectral methods for climatic time series. Reviews of geophysics, 40(1), pp.3-1, 2002.

Glick, N., Breaking records and breaking boards. The American Mathematical Monthly, 85(1), pp.2-26, 1978.

Glienke, S., Kostinski, A.B., Shaw, R.A., Larsen, M.L., Fugal, J.P., Schlenczek, O. and Borrmann, S., Holographic observations of centimeter-scale nonuniformities within marine stratocumulus clouds. Journal of the Atmospheric Sciences, 77(2), pp.499-512, 2020.

Gluhovsky, A. and Agee, E., On the analysis of atmospheric and climatic time series. Journal of applied meteorology and climatology, 46(7), pp.1125-1129, 2007.

Hansen, J., Ruedy, R., Sato, M. and Lo, K. Global Surface Temperature Change. Rev. Geophys. 48, RG4004, https://doi.org/10.1029/2010rg000345, 2010.

Hartmann, D.L., Tank, A.M.K., Rusticucci, M., Alexander, L.V., Brönnimann, S., Charabi, Y.A.R., Dentener, F.J., Dlugokencky, E.J., Easterling, D.R., Kaplan, A. and Soden, B.J., Observations: atmosphere and surface. In Climate change 2013 the physical science basis: Working group I contribution to the fifth assessment report of the intergovernmental panel on climate change (pp. 159-254). Cambridge University Press, 2013.

Haumann, F.A., Gruber, N. and Münnich, M., Sea-ice induced Southern Ocean subsurface warming and surface cooling in a warming climate. AGU Advances, 1(2), p.e2019AV000132, 2020.

Huang, B., Thorne, P.W., Banzon, V.F., Boyer, T., Chepurin, G., Lawrimore, J.H., Menne, M.J., Smith, T.M., Vose, R.S. and Zhang, H.M., Extended reconstructed sea surface temperature, version 5 (ERSSTv5): upgrades, validations, and intercomparisons. Journal of Climate, 30(20), pp.8179-8205, doi: 10.1175/JCLI-D-16-0836.1, 2017.

Huang, B., Thorne, P.W., Smith, T.M., Liu, W., Lawrimore, J., Banzon, V.F., Zhang, H.M., Peterson, T.C. and Menne, M., Further exploring and quantifying uncertainties for extended reconstructed sea surface temperature (ERSST) version 4 (v4). Journal of Climate, 29(9), pp.3119-3142, 2016.

Jordan, C., Calculus of Finite Differences, Budapest (1939); Repr. Chelsea Publ. Co., Inc., New York, 1950.

Josey, S.A., Hirschi, J.J.M., Sinha, B., Duchez, A., Grist, J.P. and Marsh, R., The recent Atlantic cold anomaly: Causes, consequences, and related phenomena. Annual Review of Marine Science, 10, pp.475-501, 2018.

Keil, P., Mauritsen, T., Jungclaus, J., Hedemann, C., Olonscheck, D. and Ghosh, R., Multiple drivers of the North Atlantic warming hole. Nature Climate Change, 10(7), pp.667-671, 2020.

Kostinski, A. and Anderson, A., Spatial patterns of record-setting temperatures. Journal of Environmental Statistics, 6(6), p.1., 2014.

Krug, J. and Jain, K., Breaking records in the evolutionary race. Physica A: Statistical Mechanics and its Applications, 358(1), pp.1-9, 2005.

Laufkötter, C., Zscheischler, J. and Frölicher, T.L., High-impact marine heatwaves attributable to human-induced global warming. Science, 369(6511), pp.1621-1625, 2020.

Lehmann, J., Coumou, D. and Frieler, K., Increased record-breaking precipitation events under global warming. Climatic Change, 132(4), pp.501-515, 2015.

Lehmann, J., Mempel, F. and Coumou, D., Increased occurrence of record-wet and record-dry months reflect changes in mean rainfall. Geophysical Research Letters, 45(24), pp.13-468, 2018.

Llovel, W., Purkey, S., Meyssignac, B. et al. Global ocean freshening, ocean mass increase and global mean sea level rise over 2005–2015. Sci Rep 9, 17717, https://doi.org/10.1038/s41598-019-54239-2, 2019.

Masson-Delmotte, V., Zhai, P., Pirani, A., Connors, S.L., Péan, C., Berger, S., Caud, N., Chen, Y., Goldfarb, L., Gomis, M.I. and Huang, M. Climate Change 2021: The Physical Science Basis. Contribution of Working Group I to the Sixth Assessment Report of the Intergovernmental Panel on Climate Change. IPCC: Geneva, Switzerland., 2021.

Myhre, G., Alterskjær, K., Stjern, C.W. et al. Frequency of extreme precipitation increases extensively with event rareness under global warming. Sci Rep 9, 16063, https://doi.org/10.1038/s41598-019-52277-4, 2019.

Oliver, E.C., Donat, M.G., Burrows, M.T., Moore, P.J., Smale, D.A., Alexander, L.V., Benthuysen, J.A., Feng, M., Gupta, A.S., Hobday, A.J. and Holbrook, N.J., Longer and more frequent marine heatwaves over the past century. Nature communications, 9(1), pp.1-12, 2018.

Pendergrass, A. G. & Hartmann, D. L. Changes in the Distribution of Rain Frequency and Intensity in Response to Global Warming. J. Climate 27, 8372–8383, https://doi.org/10.1175/jcli-d-14-00183.1, 2014.

Rahmstorf, S., Box, J.E., Feulner, G., Mann, M.E., Robinson, A., Rutherford, S. and Schaffernicht, E.J., Exceptional twentieth-century slowdown in Atlantic Ocean overturning circulation. Nature climate change, 5(5), pp.475-480, doi:10.1038/nclimate2554, 2015.

Redner, S. and Petersen, M.R., Role of global warming on the statistics of record-breaking temperatures. Physical Review E, 74(6), p.061114, 2006.

Shcherbakov, R., Davidsen, J. and Tiampo, K.F., Record-breaking avalanches in driven threshold systems. Physical Review E, 87(5), p.052811, 2013.

Van Aalsburg, J., Newman, W.I., Turcotte, D.L. and Rundle, J.B., Record-breaking earthquakes. Bulletin of the Seismological Society of America, 100(4), pp.1800-1805, 2010.

Vogel, R.M., Zafirakou-Koulouris, A. and Matalas, N.C., Frequency of record-breaking floods in the United States. Water Resources Research, 37(6), pp.1723-1731, 2001.

https://doi.org/10.5194/acp-2022-316
Preprint. Discussion started: 2 June 2022


Atmospheric Chemistry and Physics Discussions

Watson, C., White, N., Church, J. et al. Unabated global mean sea-level rise over the satellite altimeter era. Nature Clim Change 5, 565–568, https://doi.org/10.1038/nclimate2635, 2015.

Wergen, G., Bogner, M. and Krug, J., Record statistics for biased random walks, with an application to financial data. Physical Review E, 83(5), p.051109, 2011.

Wilcox, R.R., Applying contemporary statistical techniques. Elsevier, 2003.

Wuebbles, D.J., Fahey, D.W. and Hibbard, K.A., Climate science special report: fourth national climate assessment, volume I, 2017.

Yoder, M. R., Turcotte, D. L., and Rundle, J. B.: Record-breaking earthquake intervals in a global catalogue and an aftershock sequence, Nonlin. Processes Geophys., 17, 169–176, https://doi.org/10.5194/npg-17-169-2010, 2010.

https://doi.org/10.5194/acp-2022-316
Preprint. Discussion started: 2 June 2022

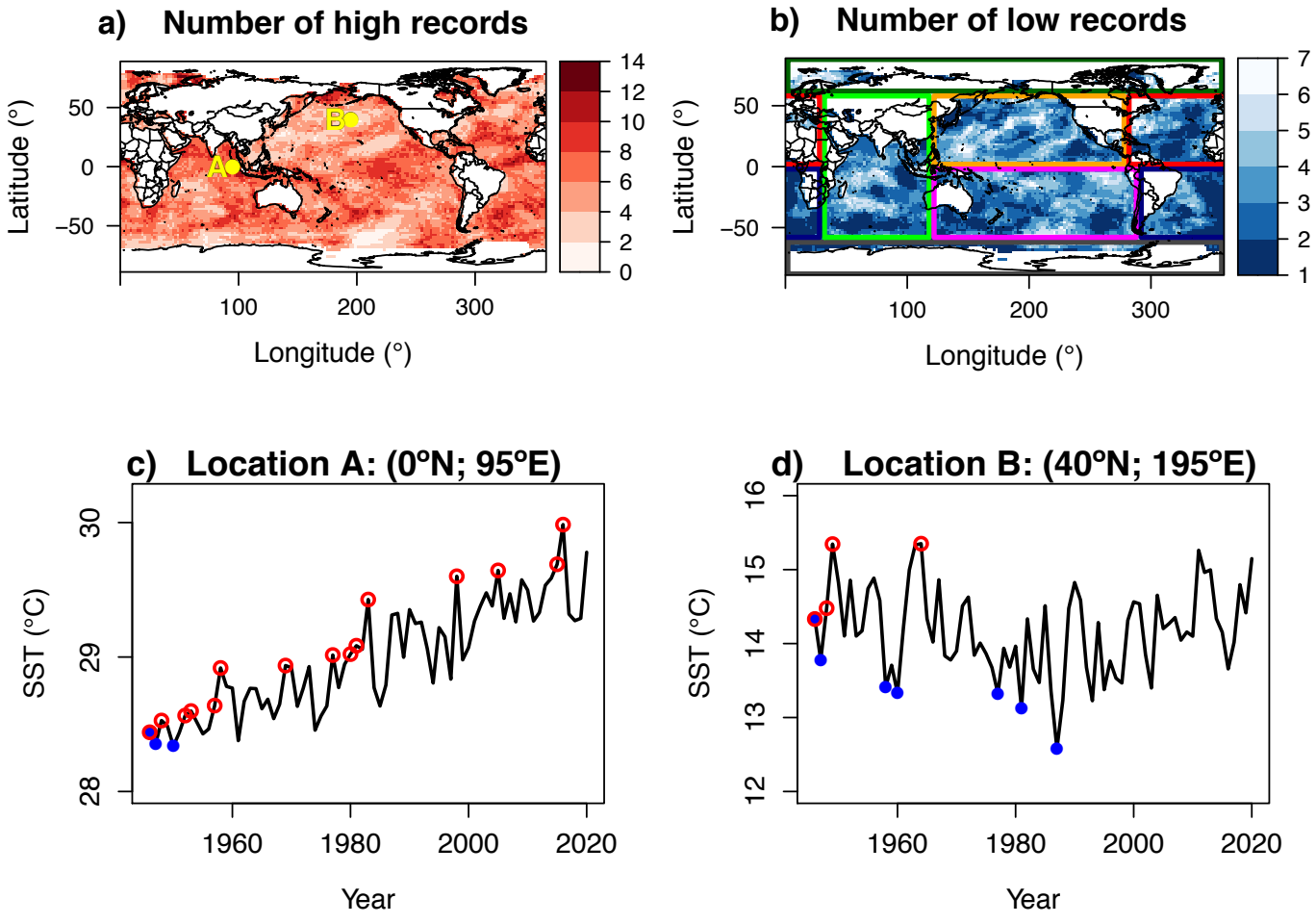

Figure 1: Number of observed high (a) and low (b) records of SST for the period between 1946 to 2020. Panels (c) and (d) show examples of time series of annual SST for two pixels, marked by yellow dots on panel (a): points A (0ºN; 95ºE) and B (40ºN; 195ºE), high/low records are marked by red/blue dots on the time series. Location A shows a clear increasing trend, with high records exceeding the low ones, while at location B, the opposite holds. The asymmetry between the number of high and low records and their deviation from the expected value for a TFRV were used to identify trends and their significance in each pixel's time series. The boxes in (b) divide the global oceans for subsequent analysis: Antarctic (ANT - gray), Arctic (ARC - dark green), Indian (IND - green), North Pacific (NP - orange), South Pacific (SP - magenta), North Atlantic (NA - red), and South Atlantic (SA - navy blue).

https://doi.org/10.5194/acp-2022-316
Preprint. Discussion started: 2 June 2022

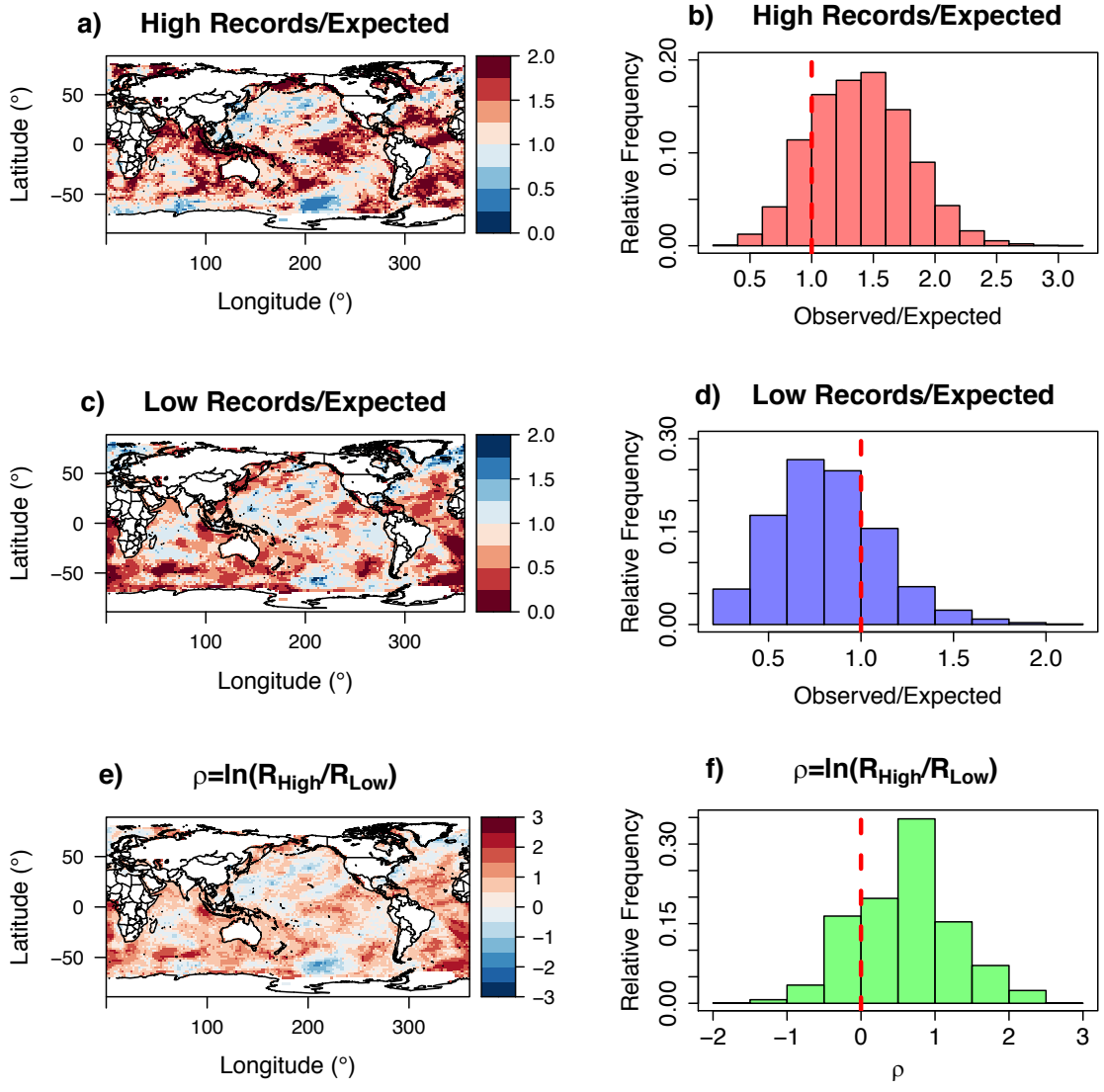

Figure 2: Number of observed high (a) and low (c) records of SST over the expected value for a TFRV in a 75-years time series. The trend indicator ρ, given by the asymmetry between the number of high and low records, $\rho = \ln(R_{High}/R_{Low})$ (e), and their respective distributions for the whole globe (b, d, f) are presented. The red dashed lines mark the thresholds where observed records exceed the expected value in (b) and (d) or when the number of high records is larger than the low records in (f). These three different indicators combined can be used to efficiently and robustly detect trends in noisy time series. The asymmetry between high and low records is evident, with a large number of high records and a small number of low records over most of the globe, particularly in the tropical and subtropical Atlantic, the Central Pacific, the eastern Indian Ocean, and the Southern sea. Note that, although the overwhelming majority of the ocean is warming, some islands of consistent cooling are observed in the maps.

https://doi.org/10.5194/acp-2022-316
Preprint. Discussion started: 2 June 2022

Atmospheric Chemistry and Physics Discussions

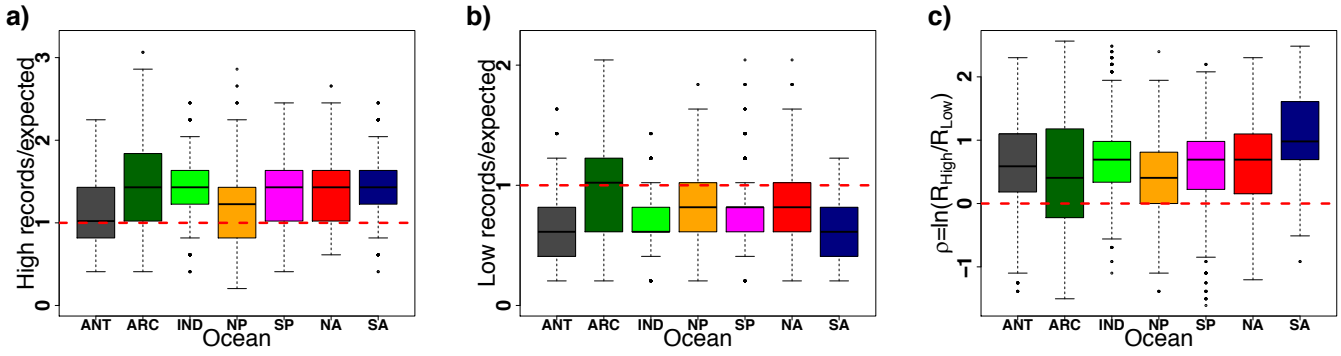

Figure 3: Box-plots of the number of high (a) and low (b) records over the expected value for a TFRV, and ρ = ln(high/low) records (c) for different oceanic regions (as marked in Fig. 1): Antarctic (ANT - gray), Arctic (ARC - dark green), Indian (IND - green), North Pacific (NP - orange), South Pacific (SP - magenta), North Atlantic (NA - red), and South Atlantic (SA - navy blue). The red dashed lines in (a,b) mark a ratio of 1 between the observed number of records and the expected value for a TFRV, and in (c) when the high records number is larger than the number of low records. An excess of high records compared to both the expected value for a TFRV and to low records is observed for all regions. The South Atlantic Ocean exhibits the largest ratio between high and low records.

https://doi.org/10.5194/acp-2022-316
Preprint. Discussion started: 2 June 2022

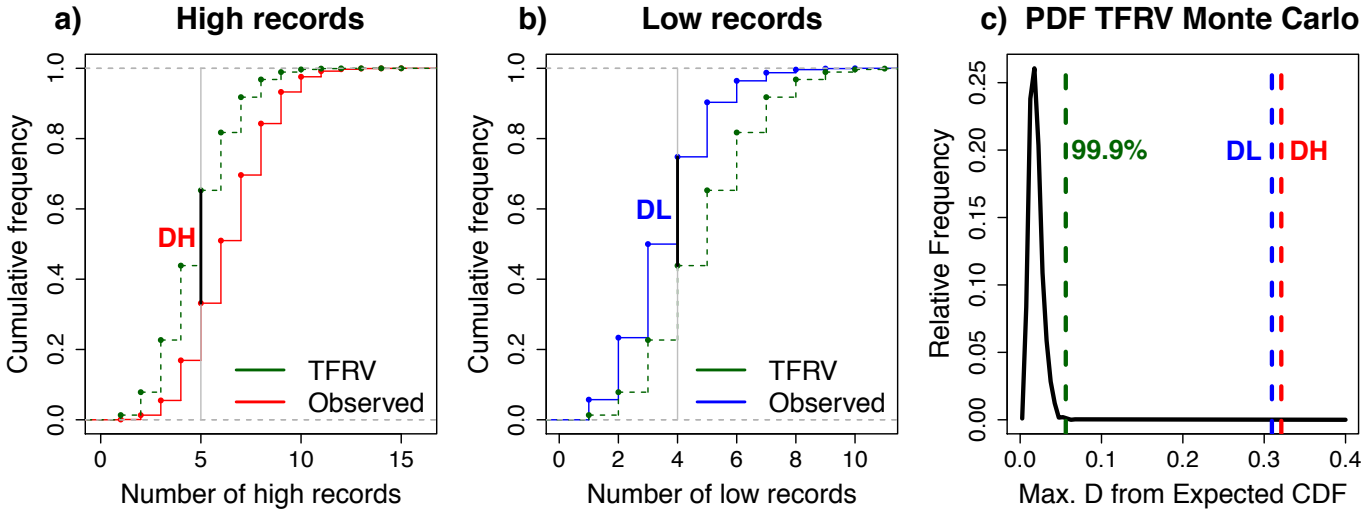

Figure 4: Cumulative distribution functions (CDFs) of the theoretical TFRV number of records from Eq. (3) (in green) and number of observed high (red) (a), and low (blue) (b) records. The Kolmogorov-Smirnov test was applied to the distributions, and the maximum distances, DH and DL, were obtained for the high and low records, respectively (black vertical lines). Notice that the exact theoretical distribution of the number of records of a TFRV time series of length 75, given by Eq. (3), was used, and it is a discrete distribution (since the number of records in a time series is an integer > 0). The probability distribution function of the maximum distance D for Monte Carlo simulations of the number of records of TFRV (c) was used to assess the significance of the results. The 99.9% percentile and the maximum deviations, DH and DL, are shown in green, red, and blue dashed lines, respectively. Both DH and DL are far above the 99.9% percentile, demonstrating the high statistical significance of SST global trends in high and low records.

https://doi.org/10.5194/acp-2022-316
Preprint. Discussion started: 2 June 2022

Atmospheric Chemistry and Physics Discussions

400

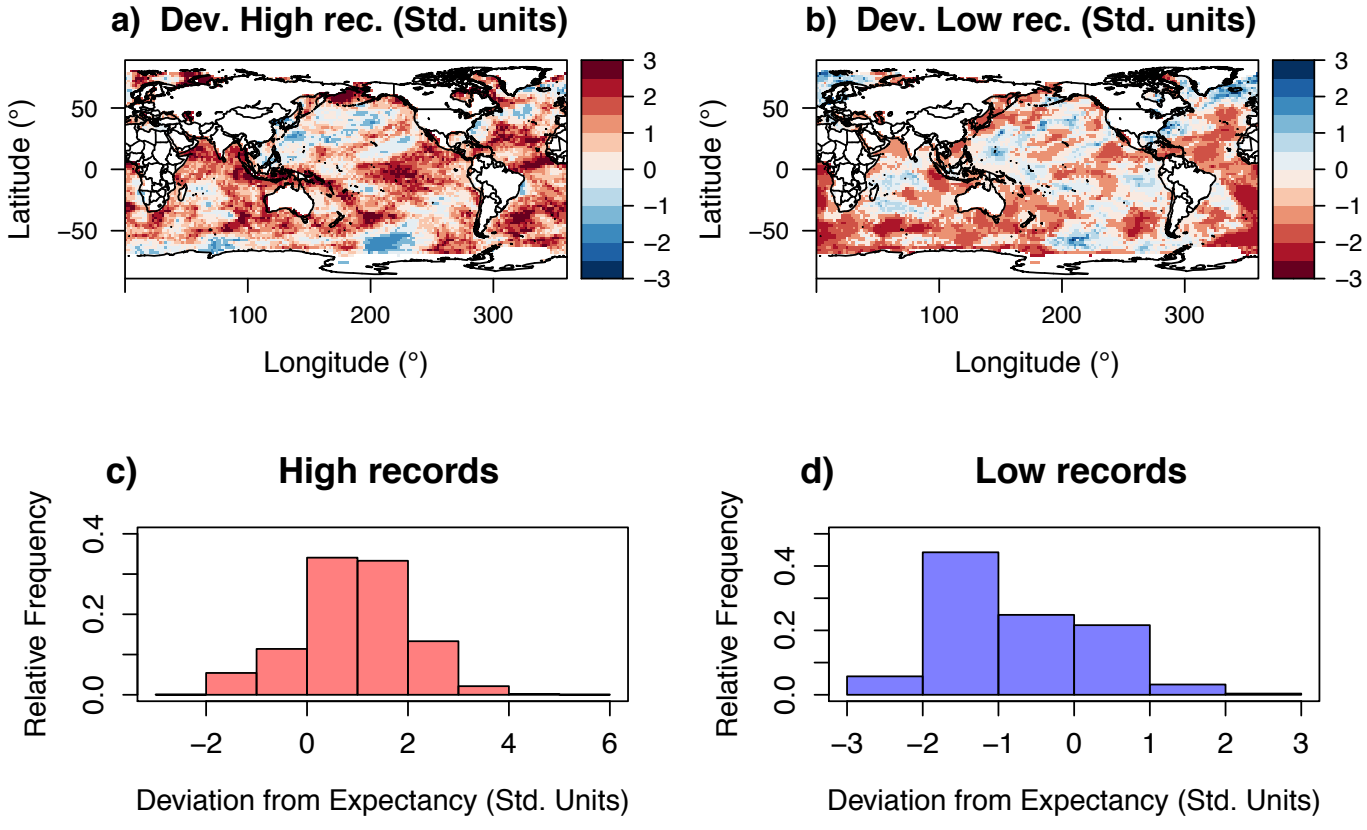

Figure 5: Departure of the observed number of high (a) and low (b) records from expectation, in units of standard deviation, and their frequency distributions (c and d). In 15.8% of the pixels, the number of high records exceeds 2 standard deviations
405 above expectation. This value is about 12 times as many pixels with that property for a TFRV and is very unlikely to result from a TFRV time series. Large deviations are observed over all the oceans for high records and predominantly in the Arctic and Atlantic Oceans for low records.